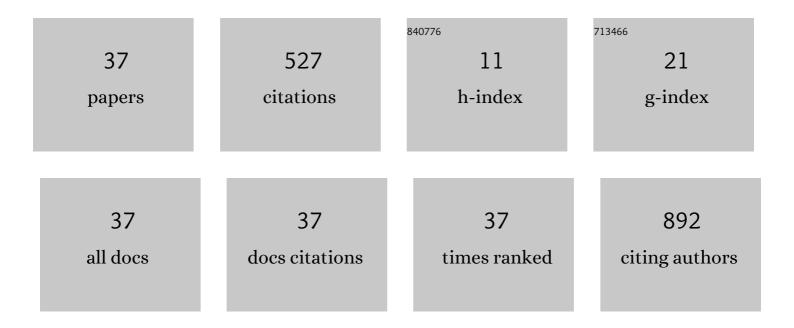
## Yu-Chun Lin

List of Publications by Year in descending order

Source: https://exaly.com/author-pdf/881096/publications.pdf Version: 2024-02-01



YII-CHIIN LIN

#	Article	IF	CITATIONS
1	Deep learning for fully automated tumor segmentation and extraction of magnetic resonance radiomics features in cervical cancer. European Radiology, 2020, 30, 1297-1305.	4.5	58
2	Dynamic contrast-enhanced MRI, diffusion-weighted MRI and 18F-FDG PET/CT for the prediction of survival in oropharyngeal or hypopharyngeal squamous cell carcinoma treated with chemoradiation. European Radiology, 2016, 26, 4162-4172.	4.5	55
3	Clinical Utility of Multimodality Imaging with Dynamic Contrast-Enhanced MRI, Diffusion-Weighted MRI, and 18F-FDG PET/CT for the Prediction of Neck Control in Oropharyngeal or Hypopharyngeal Squamous Cell Carcinoma Treated with Chemoradiation. PLoS ONE, 2014, 9, e115933.	2.5	53
4	Endometrial cancer with cervical stromal invasion: diagnostic accuracy of diffusion-weighted and dynamic contrast enhanced MR imaging at 3T. European Radiology, 2017, 27, 1867-1876.	4.5	46
5	Telomerase activity in peripheral blood for diagnosis of hepatoma. Journal of Gastroenterology and Hepatology (Australia), 2000, 15, 1064-1070.	2.8	36
6	Diffusion radiomics analysis of intratumoral heterogeneity in a murine prostate cancer model following radiotherapy: Pixelwise correlation with histology. Journal of Magnetic Resonance Imaging, 2017, 46, 483-489.	3.4	34
7	Computer-Aided Segmentation and Machine Learning of Integrated Clinical and Diffusion-Weighted Imaging Parameters for Predicting Lymph Node Metastasis in Endometrial Cancer. Cancers, 2021, 13, 1406.	3.7	22
8	Noninvasive Monitoring of Microvascular Changes With Partial Irradiation Using Dynamic Contrast-Enhanced and Blood Oxygen Level-Dependent Magnetic Resonance Imaging. International Journal of Radiation Oncology Biology Physics, 2013, 85, 1367-1374.	0.8	17
9	Blind estimation of the arterial input function in dynamic contrastâ€enhanced MRI using purity maximization. Magnetic Resonance in Medicine, 2012, 68, 1439-1449.	3.0	16
10	Phosphomimetic Mutation of Cysteine String Protein-α Increases the Rate of Regulated Exocytosis by Modulating Fusion Pore Dynamics in PC12 Cells. PLoS ONE, 2014, 9, e99180.	2.5	16
11	Myocardial triglyceride content at 3ÂT cardiovascular magnetic resonance and left ventricular systolic function: a cross-sectional study in patients hospitalized with acute heart failure. Journal of Cardiovascular Magnetic Resonance, 2016, 18, 9.	3.3	14
12	Deep learning based diagnosis of Parkinson's Disease using diffusion magnetic resonance imaging. Brain Imaging and Behavior, 2022, 16, 1749-1760.	2.1	13
13	Drosophila Model for Studying Gut Microbiota in Behaviors and Neurodegenerative Diseases. Biomedicines, 2022, 10, 596.	3.2	12
14	Metabolic Volumetric Parameters in 11C-Choline PET/MR Are Superior PET Imaging Biomarkers for Primary High-Risk Prostate Cancer. Contrast Media and Molecular Imaging, 2018, 2018, 1-10.	0.8	11
15	Prognostic model based on magnetic resonance imaging, whole-tumour apparent diffusion coefficient values and HPV genotyping for stage IB-IV cervical cancer patients following chemoradiotherapy. European Radiology, 2019, 29, 556-565.	4.5	11
16	The Prognostic Values of Leukocyte Rho Kinase Activity in Acute Ischemic Stroke. BioMed Research International, 2014, 2014, 1-11.	1.9	10
17	<sup>1</sup> H MR spectroscopy in cervical carcinoma using external phase array body coil at 3.0 Tesla: Prediction of poor prognostic human papillomavirus genotypes. Journal of Magnetic Resonance Imaging, 2017, 45, 899-907.	3.4	10
18	Fixel-Based Analysis of White Matter Degeneration in Patients With Progressive Supranuclear Palsy or Multiple System Atrophy, as Compared to Parkinson's Disease. Frontiers in Aging Neuroscience, 2021, 13, 625874.	3.4	10

Yu-Chun Lin

#	Article	IF	CITATIONS
19	Tract-Based Spatial Statistics: Application to Mild Cognitive Impairment. BioMed Research International, 2014, 2014, 1-8.	1.9	9
20	Developing and validating a multivariable prediction model to improve the diagnostic accuracy in determination of cervical versus endometrial origin of uterine adenocarcinomas: A prospective MR study combining diffusionâ€weighted imaging and spectroscopy. Journal of Magnetic Resonance Imaging, 2018, 47, 1654-1666.	3.4	9
21	Left Ventricular Function and Myocardial Triglyceride Content on 3T Cardiac MR Predict Major Cardiovascular Adverse Events and Readmission in Patients Hospitalized with Acute Heart Failure. Journal of Clinical Medicine, 2020, 9, 169.	2.4	9
22	The effect of spatial resolution on the reproducibility of diffusion imaging when controlled signal to noise ratio. Biomedical Journal, 2019, 42, 268-276.	3.1	8
23	A Method for the Prediction of Clinical Outcome Using Diffusion Magnetic Resonance Imaging: Application on Parkinson's Disease. Journal of Clinical Medicine, 2020, 9, 647.	2.4	7
24	Prediction of the Clinical Severity of Progressive Supranuclear Palsy by Diffusion Tensor Imaging. Journal of Clinical Medicine, 2020, 9, 40.	2.4	6
25	Renal perfusion assessment using magnetic nanoparticles with 7T dynamic susceptibility contrast MRI in rats. Journal of Magnetism and Magnetic Materials, 2019, 475, 76-82.	2.3	5
26	Fixel-Based Analysis Effectively Identifies White Matter Tract Degeneration in Huntington's Disease. Frontiers in Neuroscience, 2021, 15, 711651.	2.8	5
27	Early Response Monitoring Following Radiation Therapy by Using [18F]FDG and [11C]Acetate PET in Prostate Cancer Xenograft Model with Metabolomics Corroboration. Molecules, 2017, 22, 1946.	3.8	4
28	Presynaptic SNAP-25 regulates retinal waves and retinogeniculate projection via phosphorylation. Proceedings of the National Academy of Sciences of the United States of America, 2019, 116, 3262-3267.	7.1	4
29	Clinical impact of a deep learning system for automated detection of missed pulmonary nodules on routine body computed tomography including the chest region. European Radiology, 2022, 32, 2891-2900.	4.5	4
30	Early Imaging Biomarker of Myocardial Glucose Adaptations in High-Fat-Diet-Induced Insulin Resistance Model by Using 18F-FDG PET and [U-13C]glucose Nuclear Magnetic Resonance Tracer. Contrast Media and Molecular Imaging, 2018, 2018, 1-10.	0.8	3
31	Multimodal imaging reveals transient liver metabolic disturbance and sinusoidal circulation obstruction after a single administration of ketamine/xylazine mixture. Scientific Reports, 2020, 10, 3657.	3.3	3
32	Magnetic Resonance-Based Synthetic Computed Tomography Using Generative Adversarial Networks for Intracranial Tumor Radiotherapy Treatment Planning. Journal of Personalized Medicine, 2022, 12, 361.	2.5	3
33	Predictive value of 1H MR spectroscopy and 18F-FDG PET/CT for local control of advanced oropharyngeal and hypopharyngeal squamous cell carcinoma receiving chemoradiotherapy: a prospective study. Oncotarget, 2017, 8, 115513-115525.	1.8	2
34	Seroepidemiology for measles among elementary school children in Northern Taiwan. Journal of Microbiology, Immunology and Infection, 2016, 49, 561-566.	3.1	1
35	IVIM Parameters on MRI Could Predict ISUP Risk Groups of Prostate Cancers on Radical Prostatectomy. Frontiers in Oncology, 2021, 11, 659014.	2.8	1
36	Helical computed tomography of the abdomen: evaluation of image quality using 1.0, 1.3, and 1.5 pitches. Chang Gung Medical Journal, 2002, 25, 104-9.	0.7	0

#	Article	IF	CITATIONS
37	Contrast-enhanced carotid magnetic resonance angiography: comparison of single-dose and double-dose of gadolinium using the randomly segmented central k-space ordering technique. Chang Gung Medical Journal, 2005, 28, 485-91.	0.7	О